Measurement of the ^{236}U(n,f) cross-section between 4 and 10 MeV with Micromegas detectors

V. Michalopoulou, M. Diakaki, A. Stamatopoulos, A. Kalamara, M. Kokkoris, A. Lagoyannis, N. Patronis, A. Tsinganis, R. Vlastou

Measurement of the ^{236}U(n,f) cross section at fast neutron energies with Micromegas Detectors

M. Diakaki[1,2,*], *V.* Michalopoulou[3,2,**], *A.* Tsinganis[3], *A.* Axiotis[4], *A.* Kalamara[2], *M.* Kokkoris[2], *A.* Lagoyiannis[4], *N.* Patronis[5], *A.* Stamatopoulos[2], and *R.* Vlastou[2]

[1]CEA, DEN, DER/SPRC/LEPh, Cadarache, F-13108 Saint Paul Lez Durance, France
[2]National Technical University of Athens, Greece
[3]European Organization for Nuclear Research (CERN), Switzerland
[4]National Centre for Scientific Research 'Demokritos', Greece
[5]University of Ioannina, Greece

Abstract. In the present work, the measurement of the ^{236}U(n,f) cross section was performed, with reference to the ^{238}U(n,f) reaction. The measurements took place at the neutron beam facility of the National Centre for Scientific Research "Demokritos" (Greece) and the quasi-monoenergetic neutron beams were produced via the ^{2}H(d,n)^{3}He reaction in the energy range 4 – 10 MeV. Five actinide targets (two ^{236}U, two ^{238}U and one ^{235}U) and the corresponding Micromegas detectors for the detection of the fission fragments were used. Detailed Monte Carlo simulations were performed, on one hand for the study of the neutron flux and energy distribution at the position of each target, and on the other hand for the study of the energy deposition of the fission fragments in the active volume of the detector. The mass and homogeneity of the actinide targets were experimentally determined via alpha spectroscopy and the Rutherford Backscattering Spectrometry, respectively. The experimental procedure, the analysis, the methodology implemented to correct for the presence of parasitic neutrons and the cross section results will be presented and discussed.

1 Introduction

The accurate knowledge of neutron-induced cross sections is of great importance for the study and design of new generation reactors. Specifically, the isotope ^{236}U becomes important in the ^{232}Th/^{233}U fuel cycle when the fuel experiences the high burn-up chain (^{234}U -> ^{235}U -> ^{236}U, via sequential (n,γ) reactions), and acts as ^{242}Pu in the conventional uranium cycle. Thus, its fission cross section is required with 5% accuracy ([1],[2]). However, in the energy range 4 - 10 MeV few available data sets exist in literature, leading to discrepancies between the latest evaluations up to 9%.

The most recent measurement has been performed by Tovesson *et al.* [3] with the neutron time-of-flight method at LANSCE (Los Alamos). The rest of the measurements have been performed several decades ago with quasi-monoenergetic neutron beams by Meadows [4] and White and Warner [5] and in a wide energy range by Rosler *et al.* [6] and Henkel [7]. The measurements by Tovesson *et al.*, Meadows and Rosler *et al.* are in overall good agreement with each other, although above 7 MeV the data from Rosler *et al.* deviate from the other two measurements and the differences go up to 40%. The data from Henkel are systematically lower from the other data sets.

In the present work, new measurements were performed in the energy range 4 - 10 MeV and are presented here. The measurement took place at the neutron beam facility of the National Centre for Scientific Research "Demokritos" (Greece). The quasi-monoenergetic neutron beams were produced via the ^{2}H(d,n)^{3}He reaction at several neutron energies in the energy range 4 - 10 MeV. A first exploratory experiment was previously performed [8], in order to establish the analysis methodology and new measurements were performed in this energy range.

2 Experimental

2.1 Neutron production facility

The experiment was performed at the neutron beam facility of the National Centre for Scientific Research "Demokritos" using the 5.5 MV Van de Graaff Tandem accelerator. In this facility, the quasi-monoenergetic neutron beams are produced via nuclear reactions of accelerated ions, impinging on gas or solid targets. The measurements in the context of the present work were performed with neutron beams produced via the ^{2}H(d,n) reaction. A deuterium gas target fitted with 5 μm Mo entrance foil and 1 mm Pt beam stop is bombarded with a deuteron beam of the appropriate energy. The gas cell has a total length of 3.7 cm and a diameter of 1 cm, and is typically pressurized to $\approx$ 1.2 atm.

*e-mail: maria.diakaki@cea.fr
**e-mail: veatriki.michalopoulou@cern.ch

Several factors affect the monochromaticity and the fluence of the neutron beam, such as i) the energy straggling of the deuteron beam from the interaction with the Mo foil and the deuteron atoms in the gas cell, ii) the ^{2}H(d,n) reaction kinematics (very small effect to the neutron energy distribution for this target-to-gas cell distance, because the angular acceptance is less than ≈6° for all targets), iii) deuteron-induced reactions in the materials of the collimation system and/or the gas cell, producing neutrons with energies different than the main beam, iv) scattering of the neutron beam in the surrounding materials of the targets and v) the deuteron breakup reaction which creates lower energy neutrons for $E_d \geq 4.45$ MeV. The energy rippling of the deuteron beam did not exceed 4 keV, having a negligible effect on the monochromaticity of the produced neutron beam.

When the cross section measurement of interest corresponds to a non-threshold reaction, or a reaction with a significant cross section value in a wide neutron energy range, such as fission, and in the absence of a time-of-flight technique, a thorough investigation of the impact of these factors on the monochromaticity and fluence of the neutron beam is essential. This investigation is presented in Sect. 3.

2.2 Detection setup

The detection system consisted of a stack of ionisation gas cells based on the Micromegas Microbulk technology [9, 10] for the detection of the fission fragments (FF), each one containing one actinide target, the backing of which served as the detector drift electrode. In total, 5 actinide targets were used, placed in an aluminium chamber filled with a mixture of 80% Ar - 20% CO_2 kept at approximately atmospheric pressure and room temperature. Two ^{236}U targets were put back to back and two ^{238}U targets before and after them for monitoring the neutron fluence. Finally, a ^{235}U target was used, as a very sensitive tool to low energy neutron background. The experimental setup is described in more detail in [8], while a photo of the target assembly can be seen in Fig. 1. The actinide targets, in the form of thin disks of uranium oxides were manufactured via the painting technique and provided by the Institute of Physics and Power Engineering, Obninsk, and the Joint Institute of Nuclear Research, Dubna.

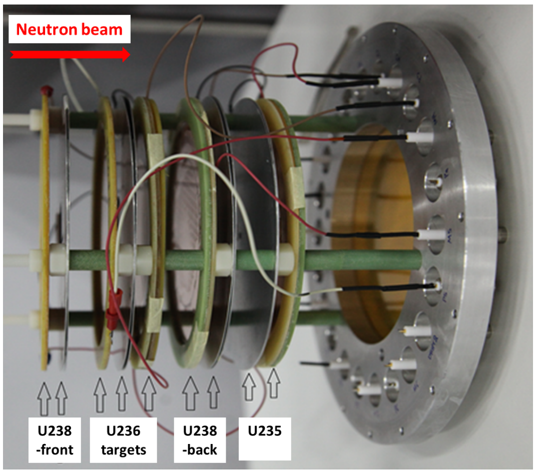

Figure 1. Photo of the target-detector assembly. The arrows show the targets and the corresponding detectors. The two ^{236}U targets were put back to back.

3 Analysis

3.1 Cross section calculation

For each incident neutron energy, the cross section of the ^{236}U(n,f) reaction was calculated relative to the ^{238}U(n,f) reaction, via the expression

$$\sigma_{U6} = \frac{Y_{U6}}{Y_{U8}} \cdot \frac{f_{U6}^{in/out}}{f_{U8}^{in/out}} \cdot \frac{f_{U6}^{par}}{f_{U8}^{par}} \cdot \frac{f_{U6}^{amp.cut}}{f_{U8}^{amp.cut}} \cdot \frac{\Phi_{U8}}{\Phi_{U6}} \cdot \frac{N_{U8}}{N_{U6}} \cdot \sigma_{U8}$$

where Y are the FF counts recorded by the detectors and corrected for i) the parasitic counts induced by neutrons of lower energies than the main neutron beam, generated from deuteron reactions at the structural materials of the gas cell and beam line ($f^{in/out}$) and from the other sources described in sec 2.1 (f^{par}) and ii) the amplitude cut introduced in the analysis ($f^{amp.cut}$). Φ is the neutron fluence of the main energy peak for each target estimated via Monte Carlo simulations, N is the areal density of each target and σ_{U8} is the cross section of the ^{238}U(n,f) reaction for each neutron energy. The determination of each of these terms is described in the following sections.

3.1.1 Estimation of fission counts and correction factors

A typical pulse height spectrum from a ^{236}U target is shown in Fig. 2. Both the alpha peak from the radioactivity of the targets and the FF are present in the spectrum. The FF counts (Y) are deduced from the integration of the spectrum, choosing carefully the integration limits from beam off spectra, in order to exclude all alpha counts.

However, these counts include fission events produced by parasitic neutrons from deuteron-induced reactions with structural materials of the gas cell and the beam line. For the estimation of these events, after each run the gas cell was emptied from the deuterium gas and bombarded with the deuteron beam under the same conditions. The fission events recorded with the empty gas cell are estimated from the gas-out spectra retaining the same integration limits as the gas-in spectra for each target. These events are attributed to neutrons created from parasitic (d,n) reactions and subtracted from the events of the corresponding run, after normalisation to the same integrated incident deuteron charge. This correction ($f^{in/out}$) ranges between 6 and 25% for ^{236}U and ^{238}U targets, and between 11 and 34% for the ^{235}U target.

An additional correction required to the FF counts, is a correction for the FF which are lost under the alpha peak and need to be taken into account. This correction ($f^{amp.cut}$) is estimated by FLUKA [11, 12] simulations using the GEF code [13] as fission event generator [8]. Typically the $f^{amp.cut}$ values deduced for the different targets were of the order of 5%. The corresponding systematic uncertainty was estimated by changing the choice of threshold and was of the order of 3%, resulting in an uncertainty of ≤0.5% for the $\frac{f_{U6}^{amp.cut}}{f_{U8}^{amp.cut}}$ ratio. The experimental and simulated spectra for the fission fragments are shown in Fig. 3.

Moreover, fission fragment counts created from neutrons of energy lower than the main neutron beam need to be subtracted from the total FF counts Y. The estimation of this correction factor (f^{par}) is discussed in detail in Sect. 3.2. The systematic uncertainty at the final cross section value from this factor was estimated to be ≤2-3%.

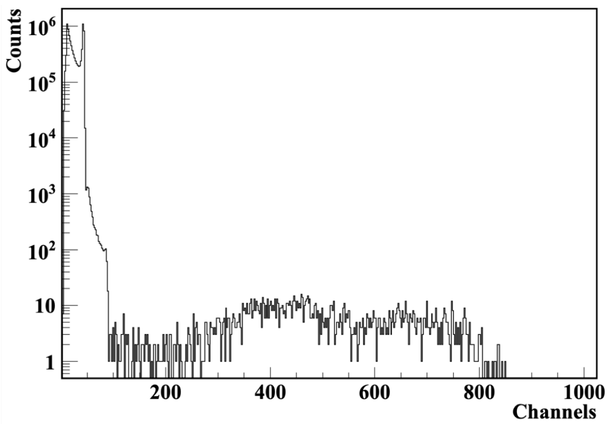

Figure 2. Experimental pulse height spectrum for ^{236}U at E_n=7.5 MeV.

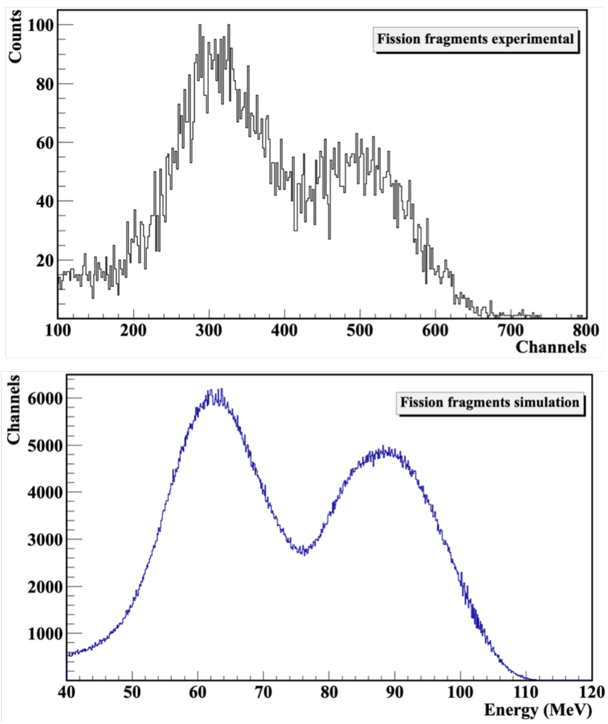

Figure 3. Experimental (upper figure) and simulated (lower figure) spectrum for the fission fragments.

3.1.2 Samples

A crucial parameter in the cross section measurements is the number of nuclei in the targets (N), and in the case of in-homogeneous neutron beams, the spatial distribution of the material on the surface of the targets. The first factor was studied with high accuracy alpha spectroscopy measurements using Silicon Surface Barrier detectors of different surfaces (described in [15]). The final mass values and the corresponding uncertainties can be found in Table 1. The contaminants of each target were determined with the same methodology and were orders of magnitude lower than the main actinide, having a negligible contribution to the FF counts.

The second factor was studied with the Rutherford Backscattering Spectrometry (RBS) technique using an external ion-beam setup (described in [15]), and it turned out that the targets were homogeneous within ≤15%. Furthermore, as mentioned above, the flux inhomogeneity due to the ^{2}H(d,n) reaction kinematics was very small, consequently the small target inhomogeneities do not affect the quality of the results.

3.2 Neutron fluence study

Detailed Monte Carlo simulations were performed implementing the neutron beam line and the detector assembly. The Monte Carlo simulations were used i) for the estimation of the neutron fluence at each target Φ, taking into account the position of the target with respect to the neutron beam and ii) for the estimation of the parasitic neutrons resulting from neutron scattering in the experimental setup and the deuteron break-up reaction for $E_d \geq 4.45$ MeV (f^{par}).

The simulations were performed with the MCNP5 code [16], using the neutron source file created from the NeuSDesc code [17]. The NeuSDesc code, coupled with SRIM-2008 [18], generates a neutron source file compatible with MCNP5. NeuSDesc takes into account the energy loss and energy and lateral straggling of the deuteron beam in the gas cell materials, the kinematics of the ^{2}H(d,n)^{3}He reaction and the deuteron break-up in the gas cell. This combination of codes has already been successfully used for the study of the neutron fluence in this facility [19].

In Fig. 4, the simulated neutron fluence at the position of the ^{236}U targets is shown for the energies of 4.5, 7.5 and 10.0 MeV. As seen in Fig. 4, apart from the main neutron energy peak, parasitic neutrons are present in the fluence and need to be accounted for in the analysis. In order to do so, the parasitic fluence, normalized to the experiment statistics, is multiplied with the cross section of each target, estimating in this way the correction factor f^{par}. The correction factor f^{par} was in the range 3-16% for the ^{238}U and ^{236}U targets, depending on the energy of the neutron beam. However, regarding the ^{235}U target the f^{par} correction factor was ranging between 5% and 21% and was not enough for the correction of the parasitic counts for the ^{235}U target. This can be explained by the high cross section of the ^{235}U(n,f) reaction in the low energy region. The parasitic neutron fluence in the region

Table 1. Summary of the target masses

	^{236}U	^{238}U	^{235}U
Diameter (cm)	8	5.2	5.2
Half life (y)	$2.342 \cdot 10^7$	$4.468 \cdot 10^9$	$7.038 \cdot 10^8$
Specific Activity (Bq/mg)	2393 ± 4	12.44± 0.01	79.98± 0.06
Mass values (mg)	5.40 ± 0.06	9.90 ± 0.13 (front)	4.96 ± 0.06
	5.01 ± 0.05	9.03 ± 0.12 (back)	
Contaminants (mg)	-	-	^{234}U($9 \cdot 10^{-5}$)

between 10^{-6} to 10^{-1} MeV seems to be underestimated by the simulations, losing parasitic counts from the neutron scattering in the experimental area, which is not included in the simulations. An estimation of the parasitic counts lost in the simulations was achieved by introducing a low energy parasitic flux in order to reproduce the experimental reaction rate of the ^{235}U target by the simulations, as shown in Fig. 5, for the run at 7.5 MeV. It is important to note that this added parasitic flux has negligible effect ($\leq$1% for all neutron energies) on the parasitic correction for the ^{238}U and ^{236}U targets, since the cross sections of the ^{236}U(n,f) and ^{238}U(n,f) reactions are very low below the fission threshold.

The estimated uncertainty of the cross section results related to the ratio $\frac{\Phi_{U8}}{\Phi_{U6}}$ was estimated from the comparison of the simulated to the experimental $\frac{\Phi_{U8-front}}{\Phi_{U8-back}}$ one and was found to be of the order of 2-3%.

Finally, the systematic uncertainty of the cross section results related to the $\frac{f^{par}_{U6}}{f^{par}_{U8}}$ correction factor was estimated by changing the shape and quantity of the parasitic tail obtained from the simulations and was found to be 0.1-2% for the different neutron energies. In addition, this ratio varied within $\leq$1% for all neutron energies, when using different evaluated libraries. Therefore, the impact of this factor at the final cross section results was found to be within their statistical errors. This can be explained by the very similar cross section shapes of the ^{238}U(n,f) and the ^{236}U(n,f) reactions, in the region where the parasitic neutrons are present, justifying the choice of ^{238}U as reference target for this experiment.

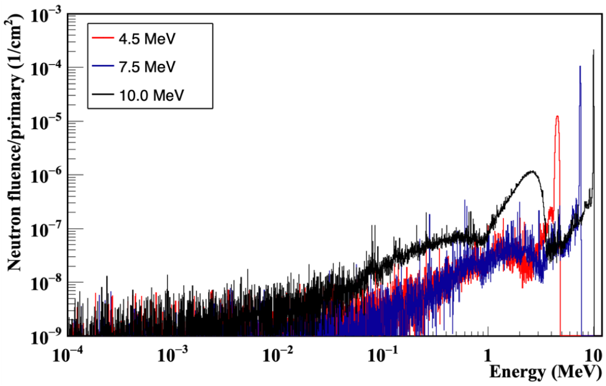

Figure 4. Simulated neutron fluence at the ^{236}U target for neutron energies 4.5, 7.5 and 10.0 MeV.

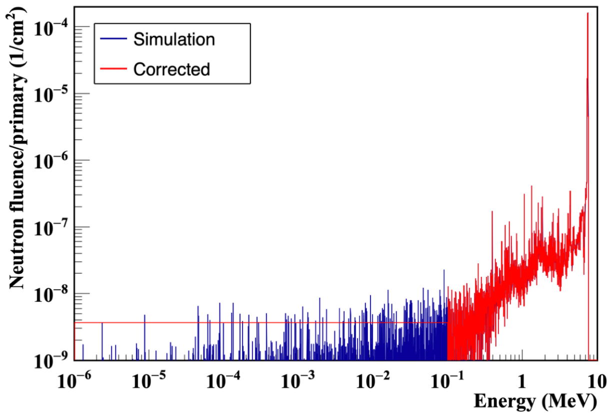

Figure 5. Simulated neutron fluence at the ^{235}U target for neutron energy 7.5 MeV and the low energy parasitic flux introduced for the correction of the simulations.

4 Results

The cross-section results obtained from the present work for the ^{236}U(n,f) reaction are presented in Table 2, along with their statistical uncertainties. The cross section presented is the weighted average value from the two ^{236}U targets. The uncertainty of the neutron energy was estimated from the full width at half maximum of the main energy peak at each neutron energy, as obtained from the Monte Carlo simulations. The main systematic uncertainties, discussed in Sect. 3, can be found in Table 3.

The cross-section results along with the existing experimental data-sets are presented in Fig. 6. The data with the symbol "r" correspond to cross section ratios ^{236}U(n,f)/^{235}U(n,f) available in EXFOR [20], converted to cross section points using the ENDF/B-VIII.0 [21] evaluation for the ^{235}U reaction (linear interpolation when needed). The results are in very good agreement with the latest data by Tovesson *et al.* and in overall good agreement with the data by Meadows. Comparing with the data by Rosler *et al.* the present measurement is in agreement within errors until the energy of 7 MeV, after which the data by Rosler *et al.* are in disagreement with all existing measurements. The data point from White and Warner at 5.4 MeV is higher by ~ 9% from the corresponding value from this work at 5.5 MeV and from the previous measurements. As mentioned in Sect. 1, the data by Henkel are systematically lower from the cross-section values of all previous measurements. Finally, the data of the ^{236}U(n,f)/^{235}U(n,f) ratio, found in EXFOR and con-

Table 2. Cross-section results for the ^{236}U(n,f) reaction.

Energy (MeV)	Cross-section (barns)
4.5 ± 0.2	0.811 ± 0.022
5.0 ± 0.1	0.787 ± 0.031
5.5 ± 0.1	0.783 ± 0.020
6.0 ± 0.1	0.887 ± 0.012
7.0 ± 0.1	1.423 ± 0.021
7.5 ± 0.1	1.511 ± 0.022
8.5 ± 0.1	1.638 ± 0.033
9.5 ± 0.1	1.558 ± 0.020
10.0 ± 0.1	1.458 ± 0.017

Table 3. Contribution of the main systematic uncertainties of the different factors to the cross section calculation

Contribution	Uncertainty (%)
Target mass	≈ 1.5%
$\frac{f_{U6}^{amp.cut}}{f_{U8}^{amp.cut}}$	<0.5%
$\frac{\Phi_{U8}}{\Phi_{U6}}$	2-3%
$\frac{f_{U6}^{par}}{f_{U8}^{par}}$	1-2%
σ_{U8}	0.7-0.95%

verted to ^{236}U(n,f) cross-section points, overall agree with the data of the present work, some of them being however systematically higher than the latter for energies below 6 MeV.

The cross-section results compared with the latest evaluations are shown in Fig. 7. As seen in this figure, for energies lower than 6 MeV the data from this work are lower than the latest evaluations from ENDF/B-VIII.0 [21], JENDL-4.0 [23] and CENDL-3.1 [24], while at this energy region the data points at 5 and 5.5 MeV are closer in value with the evaluation from JEFF-3.3, although without following the shape and values of the evaluation at the other data points. Above 6 MeV, the present work is in overall agreement with the latest evaluations, following the JENDL-4.0 and CENDL-3.1 evaluations at higher energies, which present a decrease in the cross-section values after 9.5 MeV.

5 Conclusions

The measurement of the ^{236}U(n,f) cross-section was performed, using the ^{238}U(n,f) as reference reaction with quasi-monoenergetic neutron beams at various energies in the range 4 - 10 MeV. A detailed study of the different factors in the cross section calculation was performed and presented in this contribution. The results are compared to the latest evaluations and other experimental data found in the EXFOR database. More data points are planned to be measured with the same methodology in the near future with the ^{7}Li(p,n) and ^{3}H(d,n) neutron production reactions, at lower and higher energy intervals respectively.

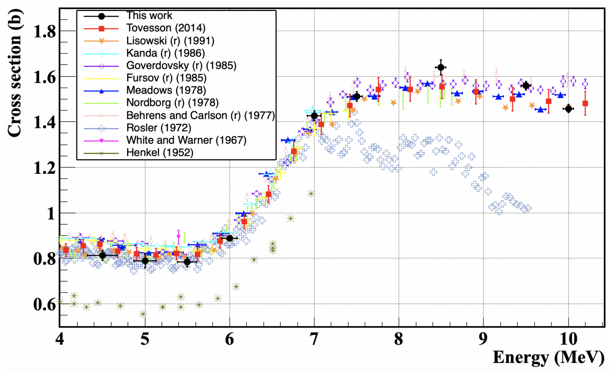

Figure 6. Cross-section results for ^{236}U(n,f) reaction (black points), along with the statistical uncertainties, in comparison to experimental datasets from EXFOR.

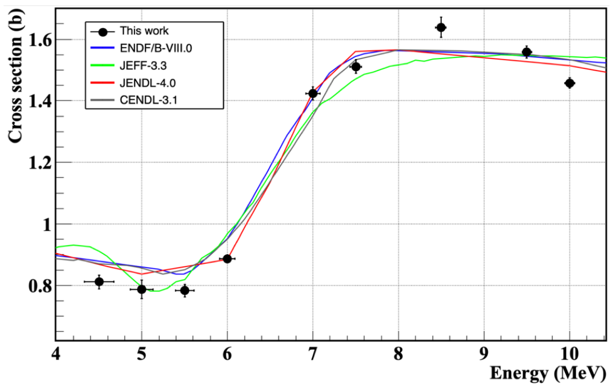

Figure 7. Cross-section results for ^{236}U(n,f) reaction (black points), statistical errors only, in comparison with the latest evaluation libraries ENDF/B-VIII.0 (blue), JEFF-3.3 (green), JENDL-4.0 (red) and CENDL-3.1 (grey).

Acknowledgements: This research is implemented through IKY scholarships programme and co-financed by the European Union (European Social Fund - ESF) and Greek national funds through the action entitled Reinforcement of Postdoctoral Researchers, in the framework of the Operational Programme Human Resources Development Program, Education and Lifelong Learning of the National Strategic Reference Framework (NSRF) 2014–2020.

References

[1] U. Abbondanno et al., “Measurements of Fission Cross Sections for the Isotopes relevant to the Thorium Fuel Cycle”, CERNINTC- 2001-025 INTC-P-145 (CERN, Geneva, 2001)

[2] V. G. Pronyaev, IAEA report No. INDC(NDS)-408 (1999)

[3] F. Tovesson et al., Nucl. Sci. and Eng. **178**, 57 (2014)

[4] J.W. Meadows, Nucl. Sci. and Eng. **65**, 171 (1978)

[5] P.H. White and G.P. Warner, Journal of Nuclear Energy **21**, 671 (1967)

[6] H. Rosler et al., Phys. Letters B **38**, 501 (1972)

[7] R.L. Henkel, Los Alamos Scientific Lab. Reports, No.1495 (1952)

[8] M. Diakaki et al., Acta Physica Polonica B **47**, No. 3 (2016)

[9] Y. Giomataris, Ph. Rebourgeard, J. P. Robert and G. Charpak, Nucl. Instrum. Methods A **376**, 29-35 (1996)

[10] S. Andriamonje et al. (The n_TOF Collaboration), Journal of the Korean Physical Society **59**, No 2, 1597-1600 (2011)

[11] A. Ferrari et al., CERN-2005-010 (2005)

[12] T.T. Böhlen et al., Nucl. Data Sheets **120**, 211 (2014)

[13] K.-H. Schmidt et al., NEA/DB/DOC(2014)1, OECD (2014)

[14] L. Waters et al., AIP Conf. Proc. 896, 91 (2007)

[15] M. Diakaki et al., Eur. Phys. J. A (2013) 49:62

[16] L. Waters et al., AIP Conf. Proc. 896, 81 (2007)

[17] E. Birgersson and G. Loevestam , Technical Report, EUR 23794 EN (European Commission, 2009)

[18] J. Ziegler, SRIM 2013, www.srim.org

[19] A. Stamatopoulos et al., Eur. Phys. J. A (2018) 54:7

[20] N. Otuka et al., Nucl. Data Sheets **148**, 1 (2018)

[21] D.A. Brown et al., Nucl. Data Sheets **120**, 272 (2014)

[22] JEFF-3.3: Evaluated Data Library 2017, http://www.oecd-nea.org/dbdata/jeff/jeff33/

[23] K. Shibata et al., Nucl. Sci. Tech. **48**, 1 (2011)

[24] Z. Ge et al., J. Korean Phys. Soc. **59**, 1052 (2011)